Journal of Applied Mechanics and Technical Physics, Vol. 48, No. 4, pp. 469–478, 2007

CONVECTIVE STRUCTURES IN A THIN LAYER OF AN EVAPORATING LIQUID UNDER AN AIRFLOW

V. P. Reutov, A. B. Ezersky, G. V. Rybushkina, and V. V. Chernov

UDC 532.526; 536.252

Evolution of convective structures in a thin layer of an evaporating liquid (ethanol) located under a turbulent boundary layer of an airflow is studied experimentally and theoretically. Evolution of the structures is examined under conditions of an increased flow velocity. A transition is found from convective cells formed in the absence of the flow to convective rolls elongated in the streamwise direction. The theoretical analysis is performed within a two-dimensional model of the flow in the liquid layer. The boundary conditions on the liquid surface are obtained with the use of self-similar solutions for mean fields in the airflow. The onset and evolution of a periodic system of rolls are simulated numerically. Theoretical conclusions are compared with experimental data.

Key words: *Rayleigh–Benard convection, shear flow, convective structures, temperature boundary layer, "cold film."*

Introduction. Convective instability caused by evaporation from a liquid surface under an air flow plays an important role in geophysical and engineering applications. Combined with radiative losses and gradient heat transfer, evaporation leads to formation of a temperature boundary layer near the surface of water basins, which is sometimes called the "cold film" [1–3]. The thickness of the temperature boundary layer depends on many factors and reaches approximately 1 mm [2, 3]. Convective rolls near the surface of water basins with a scale of several centimeters were first observed by Woodcock (as is described in [3]). The onset of the "cold film" and associated convective motion were studied by numerical simulations of energy transfer between the ocean and atmosphere [3–6]. At the same time, it is of interest to study the structures formed in the presence of the "cold film" and "wind" stresses on the liquid surface. The interest in this issue is also related to a possible convective mechanism of Langmuir circulations [1, 6].

The problem discussed can be considered as part of the global problem of convection arising in the presence of shear flows [7]. In this connection, we should note the publication [8], which describes an experimental study of convective structures in a blown-up layer of silicon oil. In that case, the effects of liquid evaporation were negligibly small (blowing resulted only in emergence of a shear flow in the liquid), and the inverse temperature distribution was generated by heating the liquid layer from below. A phenomenological model that describes convective structures in such a system was developed in [9].

The present paper describes experimental and theoretical studies of convective structures in a thin layer of an evaporating liquid under an airflow. The use of ethanol (ethyl alcohol) as a working liquid provides a more intense (as compared to water) cooling of the surface during evaporation and, moreover, does not allow adsorbing films normally observed on the water surface to form, thus, providing favorable conditions for studying convective structures.

The theoretical analysis is performed for test conditions used. The system at the initial state is assumed to be in thermal equilibrium, i.e., the airflow and the liquid have an identical temperature, and the thermal emission

Institute of Applied Physics, Russian Academy of Sciences, Nizhnii Novgorod 603950; reutov@appl.sci-nnov.ru. Translated from Prikladnaya Mekhanika i Tekhnicheskaya Fizika, Vol. 48, No. 4, pp. 3–14, July–August, 2007. Original article submitted March 28, 2006; revision submitted July 10, 2006.

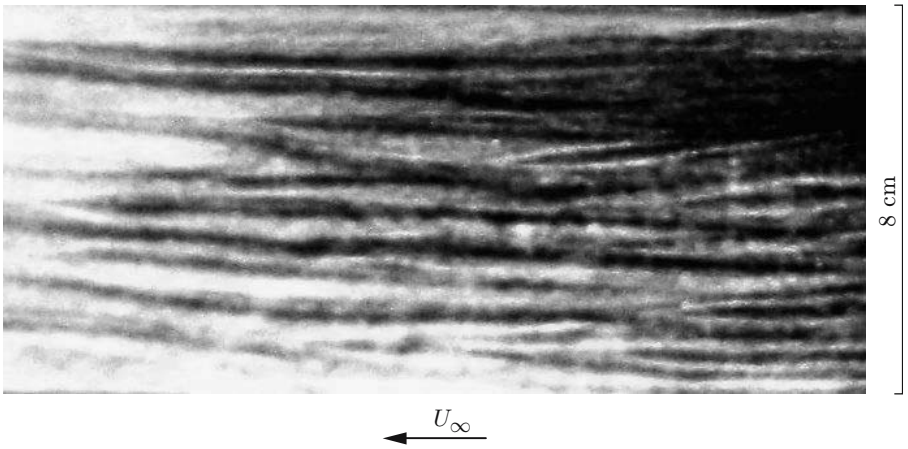

Fig. 1. Strip-like structures on the liquid surface at $U_\infty = 1.5$ m/sec (the arrow indicates the airflow direction).

of the liquid is balanced by the radiative heat flux from the ambient space. A two-dimensional model is used to describe evolution of streamwise convective rolls with axes aligned in the streamwise direction.

1. Experiment. The experiments with blowing of a liquid layer were performed in a low-turbulence wind tunnel of the Institute of Applied Physics of the Russian Academy of Sciences (30×30 cm test section 120 cm long). A Plexiglas plate containing a rectangular cavity 30 cm long and 19 cm wide was horizontally aligned in the cross section at half-height of the test section. The cavity was partly (to a depth approximately equal to 5 mm) filled by ethanol. A small part of the cavity (approximately 2 mm high) was empty to prevent liquid spillage by the airflow. The liquid in the central part of the cavity 8.2 cm wide was only contacting the airflow. The liquid on the sides of the cavity was covered by horizontal screens and separated from the flow in the central part by vertical inserts, which made the flow more uniform (see [8, 10]). The velocity of the airflow far from the plate surface was measured by an impeller anemometer. The velocity profile and its fluctuations near the surface were measured by a DISA hot-wire anemometer.

The measurements of the velocity profile showed that a turbulent boundary layer (TBL) is formed directly ahead of the cavity for free-stream velocities $U_\infty > 1.5$ m/sec. For $U_\infty = 1.5$ m/sec, the TBL thickness was $\delta \approx 2$ cm. In addition, there was a positive pressure gradient equal to 408 Pa/m above the liquid surface. The friction velocity u_* was determined by the famous Coles' approximation for the velocity profile in the TBL, combined with the dependence of the "wake force" on the pressure gradient proposed in [11]. The resultant value was $u_* = 0.05U_\infty$. The temperature of the liquid surface was measured by a radiometer by a contactless method. Simultaneously, the temperature was also measured by a thermocouple. The structures formed in the liquid were visualized by aluminum powder.

The cavity was filled by ethanol in the absence of the airflow, and a cellular structure with hexagon-like cells was formed on the surface (see [10]). In the presence of the airflow, the convective cells started elongating in the flow direction, and a system of streamwise elongated strips was formed on the liquid surface at $U_\infty \approx 0.7$ m/sec (Fig. 1). Points of branching corresponding to topological defects are clearly seen in the strip system. The mean half-period of the strips (the size of convective rolls) at the initial stage of liquid cooling is close to the depth of the layer (5 mm).

Rapid stabilization of the regime with convective rolls was followed by their slow evolution finalized by degeneration of the rolls in 15–20 min. The time evolution of the surface temperature for water and ethanol is plotted in Fig. 2 ($t = 0$ is the starting point of the airflow). The temperature gradually reaches a constant limiting value because of the overall cooling of the layer and equalization of temperature over the layer thickness. This process suppresses convective instability and makes the rolls disappear. An increase in the incoming flow velocity U_∞ leads to a certain increase in the limiting temperature, which is more substantial for alcohol.

The velocity of the steady drift flow on the liquid surface v_d was measured with the aid of video filming of motion of the wettable particles of a passive admixture applied onto the surface. At the stage of cell elongation,

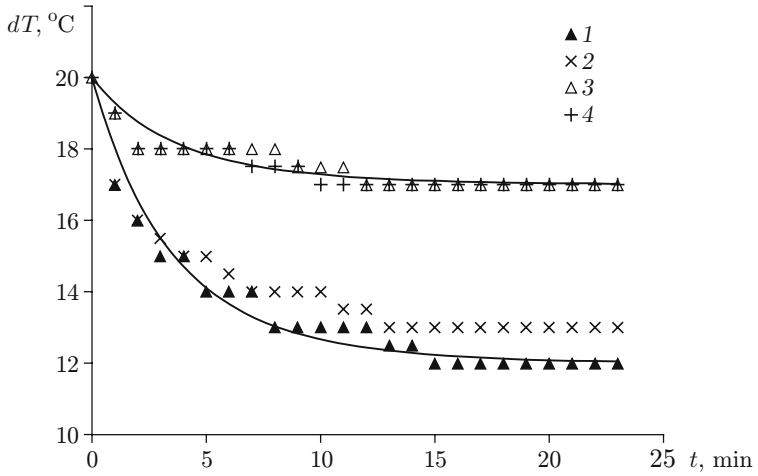

Fig. 2. Temperature of the liquid surface dT versus time for ethanol (1 and 2) and distilled water (3 and 4); $U_\infty = 1.5$ (1 and 3) and 2.5 m/sec (2 and 4).

this velocity is rather low (as rough estimates, $v_d \approx 0.3$ cm/sec at $U_\infty = 0.7$ m/sec). At $U_\infty = 1.5$ m/sec, the value $v_d = 3.2$ cm/sec was obtained. For the Couette flow induced in the liquid under the action of tangential stresses in the TBL at $U_\infty = 1.5$ m/sec, the calculations predict $v_d = 2.6$ cm/sec [8] (see also Sec. 3). At flow velocities higher than 4.5 m/sec, surface waves were generated in the downstream part of the cavity, owing to the evolution of "wind" instability, which prevented visualization of convective structures.

Such a transition from cellular convection to convective rolls was observed in the layer of a non-evaporating liquid (silicon oil), where the temperature inversion was provided by heating from below [8, 9]. In this case, if the flow velocity was fixed, a steady-state pattern of cells or rolls was established, supported by heat transfer from the heater. Moreover, the cells had a clearly expressed hexagonal shape. Blurring of the boundaries of hexagonal cells arising during evaporation is apparently caused by unsteadiness of evaporation in the absence of the airflow and by a small thickness of the temperature boundary layer ("cold film"). It should be noted that a similar picture of rolls structures with a period of 2.5 cm was obtained under natural conditions in [9].

2. Theoretical Model. Based on the estimates made in [8], we confine our theoretical considerations to the model of thermogravitational convection (Rayleigh–Benard convection), which prevails in open water basins. The results of the experiment described in Sec. 1 suggest that a regime of generation of streamwise convective rolls is established if the airflow velocity is sufficiently high. Therefore, we consider a two-dimensional model where the roll axes are aligned in the streamwise direction.

2.1. *Equations of the Problem and Boundary Conditions on the Layer Bottom.* Let the axes x, y, and z of the right-hand Cartesian system of coordinates be directed along the airflow, perpendicular to the airflow, and vertically upward (in the direction opposite to the force of gravity). If there are no disturbances inside the layer $0 < z < H$ (H is the layer depth), the "wind" flow generates a steady plane-parallel flow. In this case, convective motions with orientation of the roll axes in the x direction are possible (streamwise rolls). The equations for the liquid layer are written in dimensionless form in terms of the stream function ψ, vorticity Ω, and temperature deviation θ [12]:

$$\frac{1}{\mathrm{Pr}}\Big(\frac{\partial\Omega}{\partial t} + \frac{\partial\psi}{\partial z}\frac{\partial\Omega}{\partial y} - \frac{\partial\psi}{\partial y}\frac{\partial\Omega}{\partial z}\Big) = -\,\mathrm{R}\,\frac{\partial\theta}{\partial y} + \Delta\Omega, \qquad \Delta\psi = \Omega; \tag{1}$$

$$\frac{\partial\theta}{\partial t} + \frac{\partial\psi}{\partial z}\frac{\partial\theta}{\partial y} - \frac{\partial\psi}{\partial y}\frac{\partial\theta}{\partial z} = \Delta\theta; \tag{2}$$

$$\frac{1}{\mathrm{Pr}}\Big(\frac{\partial u}{\partial t} + \frac{\partial\psi}{\partial z}\frac{\partial u}{\partial y} - \frac{\partial\psi}{\partial y}\frac{\partial u}{\partial z}\Big) = \Delta u. \tag{3}$$

Here $\Delta = \partial^2/\partial y^2 + \partial^2/\partial z^2$, $\mathrm{R} = \alpha_0 g\delta T H^3/(\nu_0\chi_0)$ is the Rayleigh number, $\mathrm{Pr} = \nu_0/\chi_0$ is the Prandtl number, ν_0 is the kinematic viscosity of the liquid, χ_0 is the thermal diffusivity, α_0 is the thermal expansion coefficient, g is the

acceleration of gravity, δT is the scale of temperature variation, $\boldsymbol{v} = (u, v, w)$ is the flow velocity vector, $v = \partial\psi/\partial z$, $w = -\partial\psi/\partial y$, and $\Omega = -(\mathrm{rot}\,\boldsymbol{v})_x$. The quantities with the length dimension are normalized to H, and the time is normalized to H^2/χ_0 [12]. The dimensionless temperature deviation is $\theta = (T - T_0)/\delta T$ [T_0 is the initial absolute temperature of air and liquid and $T(y, z, t)$ is the current absolute temperature]. In the presence of a shear flow, the disturbances of the streamwise velocity differ from zero, but they do not affect the two-dimensional flow in the plane (y, z), which is actually autonomous.

We consider disturbances periodic in terms of y, representing them in the form of truncated Fourier series. For a convective flow satisfying the relations of symmetry $\psi(y, z, t) = -\psi(-y, z, t)$ and $\theta(y, z, t) = \theta(-y, z, t)$, the solution of Eqs. (1) and (2) is written in the form

$$\psi = \sum_{n=1}^{M} A_n(z, t) \sin(nk_1 y), \qquad \Omega = \sum_{n=1}^{M} K_n(z, t) \sin(nk_1 y), \tag{4}$$

$$\theta = \bar{\theta}(z, t) + \sum_{n=1}^{M} B_n(z, t) \cos(nk_1 y),$$

where A_n, B_n, and K_n are the real amplitudes of the harmonic numbered n, k_1 is the wavenumber of the first harmonic, and M is the number of harmonics taken into account. On the layer bottom, we impose the thermal insulation condition for temperature and the non-penetration and no-slip conditions for velocity:

$$z = 0: \qquad \frac{\partial\bar{\theta}}{\partial z} = 0, \quad \frac{\partial B_n}{\partial z} = 0, \quad A_n = 0, \quad \frac{\partial A_n}{\partial z} = 0, \quad n = 1, 2, \ldots, M. \tag{5}$$

2.2. *Boundary Conditions for the Mean Temperature on the Surface in the Presence of the Airflow.* The liquid surface lies under the TBL of the airflow. Correspondingly, free convection in the layer induces forced convection in the TBL. The joint solution of the equations for the liquid layer and convection in air makes numerical simulations rather complicated. In what follows, the structure of disturbances in the airflow is described by the linear approximation for both mean fields and fields oscillating in terms of y. In addition, the evolution of disturbances is assumed to be quasi-steady (derivatives with respect to time are neglected), because the calculations predict that convective instability is rapidly saturated, and then there follows quasi-steady evolution of a system of rolls (see Sec. 3). In calculating the fields in the airflow, we use a "quasi-laminar" model of the TBL flow, where a laminar flow with an identical mean velocity profile is put into correspondence to the turbulent flow.

On the liquid surface, we impose the conditions of a "rigid top," continuity of temperature, no-slip conditions, and continuity of shear stress in the form [12, 13]

$$w\Big|_{z=H\pm0} = 0, \qquad \theta\Big|_{z=H-0} = \theta\Big|_{z=H+0}, \qquad (u, v)\Big|_{z=H-0} = (u, v)\Big|_{z=H+0},$$
$$\rho_0\nu_0\Big(\frac{\partial u}{\partial z}, \frac{\partial v}{\partial z}\Big)\Big|_{z=H-0} = \rho_a\nu_a\Big(\frac{\partial u}{\partial z}, \frac{\partial v}{\partial z}\Big)\Big|_{z=H+0}, \tag{6}$$

where ρ_0 is the liquid density and ρ_a and ν_a are the air density and kinematic viscosity, respectively. Dimensionless variables are used in Eq. (6) and further in this section (if not indicated otherwise). On the liquid–air interface, the heat-flux balance equation acquires the form [1, 2]

$$-\varkappa_0 \frac{\partial\theta}{\partial z}\Big|_{z=H-0} = \Big(-\varkappa_a \frac{\partial\theta}{\partial z} + L_V\gamma[\rho_\varphi(T) - \rho(T)] + 4\varepsilon\sigma T_0^3\theta\Big)\Big|_{z=H+0}, \tag{7}$$

where $\varkappa_0$ and $\varkappa_a$ are the thermal conductivities of the liquid and air, respectively, L_V is the latent heat of evaporation, $\rho_\varphi(T)$ is the density of saturated vapor at a temperature T, $\rho(T)$ is the vapor density, γ is the rate of evaporation into vacuum, σ is the Stefan–Boltzmann constant, and ε is the radiant emittance of the liquid. In addition to gradient heat fluxes, Eq. (7) contains heat fluxes caused by evaporation and distortion of the radiative balance due to liquid-surface cooling. Note that radiative effects on the sea surface play an important role [2]. The heat flux due to evaporation in Eq. (7) is determined by the formula of the kinetic theory [14, p. 63]. The dependence of ρ_φ on temperature has the form [15, p. 200]

$$\rho_\varphi(T) = \rho_\varphi(T_0)\,\frac{T_0}{T}\,\exp\Big[\lambda_\varphi\Big(\frac{1}{T_0} - \frac{1}{T}\Big)\Big], \tag{8}$$

where $\lambda_\varphi = L_V g_m/R_*$ (g_m is the molecular weight of the liquid) and R_* is the universal gas constant. In the working range of temperatures, we replace Eq. (8) by its linear approximation

$$\rho_\varphi = \rho_\varphi(T_0)[1 + k_c(T - T_0)(\lambda_\varphi - T_0)/T_0^2] \tag{9}$$

(k_c is a correcting coefficient). By comparing the plots of the functions (8) and (9) with typical values of the parameters (see Sec. 3), we find that $k_c = 0.8$ ensures the relative error of dependence (9) within 7% in the entire working range of temperatures (the error equals zero for $k_c = 1$ and $T \to T_0$ and 35% at the edge of the working range of temperatures).

The density of saturated vapor is substantially lower than the density of air (at standard pressure and temperature of 20°C, $\rho_\varphi = 0.11$ g/cm^3 for alcohol); therefore, the vapor density $\rho(x, y, z, t)$ is described by the linear advection-diffusion equation (see [16])

$$\frac{\partial \rho}{\partial t} + U_a(z, x)\,\frac{\partial \rho}{\partial x} = D\Delta\rho. \tag{10}$$

Here D is the coefficient of diffusion of vapor in air and $U_a(z, x)$ is the airflow velocity profile. As the estimates of the problem parameters made in Sec. 3 show that the changes in temperature and vapor concentration occur in the near-wall (buffer) region of the TBL, we use the linear approximation $U_a(z, x) = (u_*^2/\nu_a)(z - H)$, where $u_*(x)$ is close to constant. The velocity of the drift flow on the layer surface can be neglected (see Sec. 3). Typical changes in the mean temperature and vapor density in the airflow direction have a scale l of the order of the cavity length, which is significantly greater than the vertical scales of vapor diffusion and heat transfer in the TBL. Taking this circumstance into account and using Eq. (10), we write the equation for the steady profile of the mean vapor density $\bar\rho(z, x)$ in dimensionless coordinates $X = x/l$ and $Y = (z-H)/l_D$, where $l_D = (\nu_a l D/u_*^2)^{1/3}$ is the scale of diffusion. Presenting the solution of this equation in the form $\bar\rho = [\rho_\varphi(T_s) - \rho_\infty]F(X, Y) + \rho_\infty$, where $T_s = T|_{Y=0}$ is the temperature on the layer surface and ρ_∞ is the vapor density in the ambient air, we obtain the equation

$$Y\,\frac{\partial F}{\partial X} = \frac{\partial^2 F}{\partial Y^2}. \tag{11}$$

The boundary condition for Eq. (11) on the plane $Y = 0$ means that the mass flux due to evaporation equals the diffusion mass transfer. Supplementing this condition by an obvious boundary condition "at infinity," we obtain

$$F - 1 = \beta\,\frac{\partial F}{\partial Y}\Big|_{Y=0}, \qquad F\Big|_{Y\to\infty} \to 0, \tag{12}$$

where $\beta = D/(\gamma l_D) \ll 1$ is a small parameters characterizing the ratio of the diffusion rate to the rate of evaporation into vacuum. The heat flux due to evaporation in Eq. (7) is proportional to $1 - F$ and equals zero in the zeroth approximation of β. In this approximation, F satisfies Eq. (11) with the boundary conditions $F|_{Y=0} = 1$ and $F|_{Y\to\infty} = 0$. Such a boundary-value problem has a self-similar solution of the form $F = \Gamma(1/3, \xi^3/9)/\Gamma(1/3)$, where $\xi = YX^{-1/3}$; the functions Γ with one and two arguments are the gamma-function and incomplete gamma-function, respectively. As $\xi \to \infty$, the function $F(\xi)$ monotonically decreases from 1 to 0 ($F = 0.035$ already at $\xi = 2.5$). The heat flux due to evaporation j_V is found by substituting the solution for F in the zeroth approximation into the right side of the first boundary condition (12): $j_V = d_1(D/l_D)[\rho_\varphi(T_s) - \rho_\infty]X^{-1/3}$. Here $d_1 = (-dF/d\xi)\Big|_{\xi=0} \approx 0.54$.

This self-similar solution was obtained for a uniform (in terms of x) distribution $\rho_\varphi(T)$ and, hence, for a constant temperature T_s. A self-similar solution with a constant heat flux is also possible. The solution with a constant temperature T_s was chosen because the function ρ_φ has a temperature-independent component [see Eq. (9)]. In addition, a constant distribution of T_s in the downstream direction was confirmed experimentally. Thus, the vapor density is close to the saturated vapor density near the surface and tends to ρ_∞ with distance from the surface.

The problem of determining the mean temperature profile in the TBL is posed similarly to the above-considered problem for vapor density [see Eq. (10)]. The solution of this problem can be presented as $T = (T_s - T_0)F(X, Y) + T_0$; in this case, $Y = (z - H)/l_T$ [$l_T = (\nu_a l \chi_a/u_*^2)^{1/3}$ and χ_a is the thermal diffusivity of air]. As F satisfies the boundary conditions $F|_{Y=0} = 1$ and $F|_{Y\to\infty} = 0$, the solution of the problem considered is the function $F(\xi)$ found above. Then, for the gradient heat flux j_T [the first term in the right side of Eq. (7)], we obtain $j_T = (d_1 \varkappa_a/l_T)(T_s - T_0)X^{-1/3}$.

For matching the resultant solutions with the two-dimensional model of convective rolls in the liquid layer, we put $X = 1$ in the expressions for j_V and j_T. The matching coordinate is determined as $x = l$. Substituting j_V

and j_T into Eq. (7), we obtain a closed boundary condition for the mean temperature on the layer surface. The scale of temperature variation is introduced as $\delta T = d_1 D L_V H \rho_\varphi(T_0)(1-\lambda_\rho)/(l_D \varkappa_0)$. Here $\lambda_\rho = \rho_\infty/\rho_\varphi(T_0)$ is the humidity of the ambient air, determined from the concentration of vapor of the evaporating liquid. This allows us to write the boundary condition for the mean temperature in dimensionless form as

$$z = 1 - 0: \qquad \frac{\partial \bar{\theta}}{\partial z} = -b\bar{\theta} - 1, \tag{13}$$

where $b = s_V + s_T + s_R$ is the coefficient of heat transfer from the surface. The quantities $s_V = k_c(\lambda_\varphi - T_0)\delta T/[(1-\lambda_\rho)T_0^2]$, $s_T = d_1 \varkappa_a H/(\varkappa_0 l_T)$, and $s_R = 4\sigma\varepsilon T_0^3 H/\varkappa_0$ determine the contributions of the temperature dependence of evaporation, gradient heat transfer, and violation of the radiative balance to the heat transfer from the surface.

Note that -1 appears in the right side of Eq. (13) because of the above-made choice of the temperature scale. The heat flux due to evaporation equal to -1 is the heat flux due to evaporation at the initial time (when $\bar{\theta} = 0$). Therefore, δT is the temperature difference over the layer thickness with a linear profile of temperature, where the heat flux inside the layer coincides with the heat flux into air at the initial time.

2.3. *Boundary Conditions for Oscillating Components of Hydrodynamic Fields.* In determining the oscillating (over the y coordinate) components of the fields, we use the same assumptions as in Sec. 2.2; moreover, we neglect the derivatives with respect to x. Using Eqs. (1) and (2) supplemented by the advection-diffusion equation for vapor density, we present their solution in the form (4) and linearize the resultant equations with respect to the mean profiles of temperature and vapor density found in Sec. 2.2 [the solution of the equation for vapor density is constructed in the same form as the solution for temperature (4)]. Using only the linear approximation of the function F, we assume that $F(\xi)\Big|_{X=1} \approx 1 - d_1 Y$. As a result, we obtain equations for the amplitudes of harmonics in air with constant coefficients. Solving this system with allowance for the boundary conditions (6) and (7), we can obtain effective boundary conditions on the liquid surface, which close the system of equations for the liquid layer.

The results of calculations with the values of parameters corresponding to conditions of experiments performed (see Sec. 3) show that the effective boundary conditions can be replaced, without losing accuracy, by simpler relations, which have the following form in dimensionless variables:

$$z = 1 - 0: \qquad \frac{dB_n}{dz} = -bB_n, \quad \frac{d^2 A_n}{dz^2} = 0, \quad A_n = 0. \tag{14}$$

The first equation in (14) is the generalization of the boundary condition (13) to the case of full temperature deviation θ, the second one implies the absence of oscillating shear stresses, and the third equation means a motionless plane boundary. The use of conditions (14) allows us to avoid the problem of determining oscillating fields in air. The calculations show (see Sec. 3) that the profiles of harmonics of the stream function and temperature in this case are close to those obtained with the use of full effective boundary conditions. A small difference in the profiles of harmonics of temperature (less than 5%) is noted only in an immediate vicinity of the surface. Note that the first condition in (14) can be replaced approximately with the same error by the condition of thermal insulation ($dB_n/dz = 0$). The calculations of the flow structure and its evolution in time with the use of full and simplified boundary conditions also yield similar results.

3. Results of Numerical Simulations. Physical parameters of alcohol, air, and alcohol vapor in air at a temperature of 20°C and standard pressure were taken from appropriate tables. The dimensionless parameters for numerical simulations were determined at $U_\infty = 1.5$ m/sec, $u_*/U_\infty = 0.05$, $H = 4.6$ mm, $l = 15$ cm (half-length of the cavity), and humidity $\lambda_\rho = 0$. These data correspond to R = 60,140 and $b = 0.68$. The Prandtl number for alcohol under these conditions is Pr = 16.6 [16]. Note that the coefficient in Eq. (8) is $\lambda_\varphi = 5120$, and the time scale is $H^2/\chi_0 = 3.7$ min.

The scales of the diffusion and thermal boundary layers in the airflow, normalized to the viscous length scale for the TBL, are $l_D u_*/\nu_a = 7.85$ and $l_T u_*/\nu_a = 10.1$. The thickness of the buffer region of the TBL on a smooth surface in the same units is usually assumed to be 30 [2]. Assuming that $X = 1$ ($\xi = Y$) and taking into account the behavior of the function $F(\xi)$, we find that heat and vapor diffusion occurs in the buffer region of the TBL. This allows us to use the linear approximation for the airflow velocity profile (see Sec. 2.2). Note also that the increment of flow velocity on the scales l_D and l_T is substantially greater than the velocity of surface drift in the liquid. For this reason, the latter can be neglected in Eq. (11).

Equations (1) and (2) with the boundary conditions (5) and (13) admit a solution in the form of a vertically uniform steady-state temperature distribution $\bar{\theta}(z) = \theta_{\rm st} = -1/b$, which is obviously stable and corresponds to cooling of the entire liquid layer. The steady-state temperature is also observed to stabilize in the experiment (see Fig. 2). The calculations yield the following values of parameters: $s_V = 0.38$, $s_T = 0.166$, $s_R = 0.131$, and $\theta_{\rm st} = -1.48$. Thus, in determining $\theta_{\rm st}$, the dependence of saturated vapor density on temperature s_V is important, though the total contribution of s_T and s_R is also significant. The difference between the initial temperature T_0 and the absolute temperature of the layer can be presented as $T_0 - T_{\rm st} = (1 - \lambda_\rho)T_0^2/[(1 + s'_T + s'_R)k_c(\lambda_\varphi - T_0)]$, where $s'_T = s_T/s_V$, $s'_R = s_R/s_V$, and $T_{\rm st} = T_0 + \delta T\,\theta_{\rm st}$ is the absolute steady-state temperature of the layer. If $s'_T \to 0$ and $s'_R \to 0$, then the decrease in temperature $T_0 - T_{\rm st}$ during layer cooling is completely determined by the dependence of saturated vapor density on temperature. It follows from the estimates made above that the limiting temperature in the experiment is expected to weakly depend on flow velocity, which is consistent with data plotted in Fig. 2.

Substituting Eq. (4) into Eqs. (1) and (2), we obtain an evolutionary boundary-value problem in partial derivatives with respect to t and z for the amplitudes of harmonics and mean temperature with the boundary conditions (5), (13), and (14). In the present paper, we consider only periodic solutions of this problem containing two convective rolls in the period. In numerical simulations, the period of the solution was set in accordance with experimental data (it was assumed that $k_1 = 3$, which corresponds to the period of rolls equal to $2.1H$). To obtain a numerical solution, we used a mesh uniform in the z direction, and the derivatives with respect to z were replaced by second-order differences. Equations in ordinary derivatives with respect to t were written for working nodes of the mesh numbered $n = 1, 2, \ldots, N$. The values of the variables in the edge nodes $n = 0, N + 1$ were determined from the boundary conditions at $z = 0$ and $z = 1$. A large system of ordinary differential equations with respect to t was integrated by the fourth-order Runge–Kutta method with a constant step. The second equation in system (1) was solved by the differential sweep method. Most calculations were performed with $N = 100$, and some calculations were performed with $N = 200$. The number of harmonics in most calculations was $M = 6$. Similar results were obtained for other values of R, k_1, and M. At the initial time, a uniform mean temperature profile $\bar{\theta} = 0$ and a small first harmonic of the stream function $A_1 = 10^{-3}\sin(m\pi z)$ (m is an integer) were specified. The remaining coefficients A_n and all coefficients B_n were assumed to be zero. The fields at the stage of quasi-steady evolution of the roll structures were found to be almost identical for $m = 1$, 2, and 3.

The calculated results are plotted in Figs. 3–5. At the initial stage of the process ($t < 0.15$), intense generation of the rolls is observed; the maximum amplitude of the first harmonic of the stream function reaches $A_1 \approx 45$. Then, the generation intensity drastically decreases, and the amplitudes of harmonics monotonically decrease to zero at $t > 0.3$ (the amplitude of velocity on the layer surface is $v \approx 40$ at $t = 0.5$). This corresponds to the stage of quasi-steady evolution of the rolls, when convective instability has been already stabilized and all changes in the flow are caused by cooling of the liquid layer. An analysis of the mean temperature profile behavior showed that liquid cooling from the surface leads first to formation of a temperature profile with a large (commensurable to unity) slope over the entire layer thickness. As the Rayleigh number is high, intense generation of convective rolls is observed.

Figure 3 shows the mean temperature profiles, which can be used to elucidate the evolution of the "cold film" and quasi-steady cooling of the layer. The "cold film" is characterized by a small but abrupt decrease in temperature near the layer surface $z = 1$. In the remaining part of the layer, the temperature changes smoothly and insignificantly. The limiting value of temperature in a uniformly cooled layer coincides with the value of $\theta_{\rm st}$ given above. The temperature scale is $\delta T = 8.5°$C, and the limiting decrease in the layer temperature is $T_0 - T_{\rm st} = 12.5°$C. As is seen in Fig. 2, in the experiment with alcohol and $U_\infty = 1.5$ m/sec, cooling was somewhat smaller (approximately 9°C). The dimensionless time of cooling is 5, i.e., 18.5 min, which is in good agreement with experimental data plotted in Fig. 2. The time evolution of surface temperature (not shown here) is also in qualitative agreement with the data in Fig. 2. The dimensionless thickness of the "cold film" is approximately 0.2, which corresponds to 1 mm. At $t = 0.5$, the temperature difference on the "cold film" is 0.075 (0.64°C). These estimates are close to available data for water basins [2].

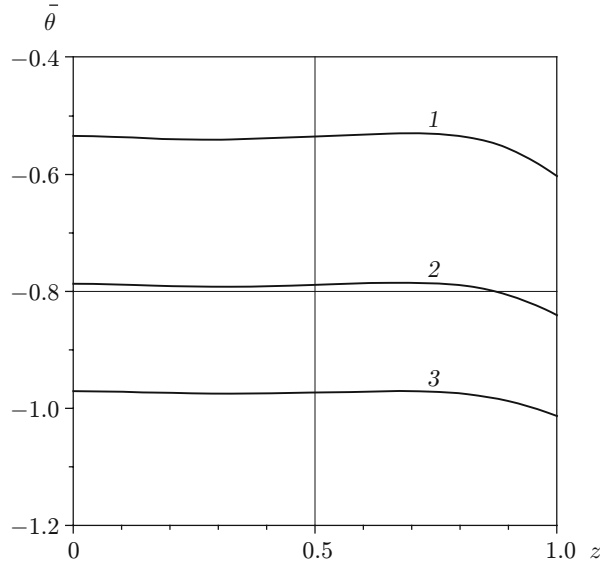

Fig. 3

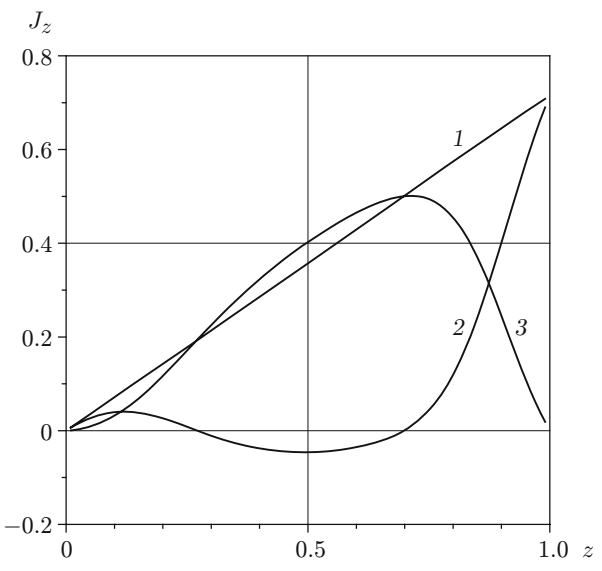

Fig. 4

Fig. 3. Mean temperature profiles inside the liquid layer under the airflow at different times (R = 60,140, Pr = 16.6, $b = 0.68$, and $k_1 = 3$): $t = 0.75$ (1), 1.25 (2), and 1.75 (3).

Fig. 4. Dimensionless heat flux in the z direction (curve 1) and its molecular component (curve 2) and dynamic component (curve 3).

According to Eq. (2), the expression for the normalized heat flux toward the surface is

$$J_z = -\frac{\partial \bar{\theta}}{\partial z} + \langle \tilde{w}\tilde{\theta} \rangle, \tag{15}$$

where the tilde corresponds to the components of temperature θ and vertical velocity w oscillating over y; $\langle \tilde{w}\tilde{\theta} \rangle$ is the mean value averaged over the period of spatial oscillations. Figure 4 shows the total heat flux (15) and its molecular and dynamic components [determined, respectively, by the first and second terms in the right side of Eq. (15)] versus the z coordinate. Prevailing of the molecular component near the surface is responsible for the large temperature gradient in the "cold film," while the large dynamic thermal conductivity generated inside the layer by convective motions restricts the film thickness. The distributions in Fig. 4 are similar to those known for turbulent boundary layers of different origin (e.g., for the turbulent flux of momentum in the TBL near the wall [2]). Thus, the small thickness and stability of the "cold film" are caused by the presence of convective structures responsible for higher dynamic thermal conductivity in the main part of the liquid layer.

Figure 5 shows the isotherms and the streamlines in the flow. The streamlines become compressed in regions of downward motion of the cold liquid and expand in regions of upward motion of the warm liquid. Thus, the cold liquid goes down in the form of thin jets, and this occurs faster than the warm liquid goes upward. The cold liquid goes downward under the lines of convergence of the surface flow. These lines pass through the points $z = 1$, $y = 0$, 2.1, and 4.2 in Fig. 5 (white stripes in Fig. 1 formed by powder particles). The warm liquid goes upward under the lines of divergence. These lines pass through the points $z = 1$, $y = 1.05$ and 3.15 in Fig. 5 (dark stripes in Fig. 1).

Equation (3) for the streamwise component of velocity was solved with the boundary conditions $\partial u/\partial z = \rho_a u_*^2 H^2/(\rho_0 \chi_0 \nu_0) \equiv C_0$ at $z = 1$ and $u = 0$ at $z = 0$. This problem is a linear boundary-value problem with variable coefficients, which has a steady-state solution of the form $u = C_0 z$ in the absence of convection. Therefore, the relative change in the mean flow velocity $\delta\bar{u} = \bar{u}/C_0 - z$ is independent of C_0. For the values of parameters used above, $C_0 = 1140$. The function $\delta\bar{u}(z)$ is monotonic; at $t = 0.5$, it has a minimum on the layer surface ($\delta\bar{u} = -0.06$ at $z = 1$) and a maximum on the bottom [$\delta\bar{u}(0) = 0$ at $z = 0$]. The streamwise velocity on the surface $u(t, y, z)|_{z=1}$ has a maximum value on the lines of convergence and a minimum value on the lines of divergence. Its crossflow oscillations at $t = 0.5$ reach 20% of velocity in the absence of convection.

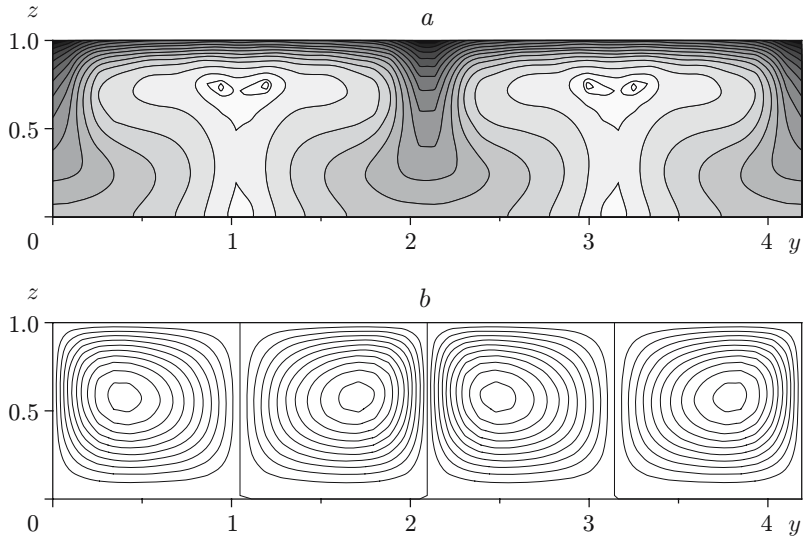

Fig. 5. Isotherms (a) and streamlines (b) of the periodic convective flow in the liquid layer under the airflow at $t = 0.5$: (a) the black and white colors refer to the minimum and maximum temperatures, respectively.

To estimate the dependence of the calculation results on the matching coordinate $x = l$ (see Sec. 2.2), we performed calculations with $l = 9$ and 23 cm (which covers almost the entire region of the liquid surface in Fig. 1). The values for $l = 9$ cm were R = 71,300, $b = 0.78$, $\delta T = 10°$C, and $T_0 - T_{\text{st}} = 12.9°$C. The corresponding values for $l = 23$ cm were R = 52,150, $b = 0.6$, $\delta T = 7.3°$C, and $T_0 - T_{\text{st}} = 12.1°$C. As determining δT depends on l (see Sec. 2.2), we first passed to a fixed scale $\delta T = 1°$C and then compared the calculated mean temperatures. The calculations for different values of l were compared in the time interval $0.5 < t < 3$ (except for the time intervals of the transitional regime and small values of the quantities considered). For $l = 9$ and 23 cm, the relative deviations of temperature on the surface layer, the temperature difference in the "cold film," and the maximum amplitude of the first harmonic of the stream functions from the values of these quantities calculated at $l = 15$ cm were within 10 and 8%, respectively. The relative deviations of the amplitude of the second harmonic were considerably smaller. Thus, the calculated results show that the hydrodynamic fields only weakly depend on the matching coordinate.

The fields of temperature and velocity of the convective flow in Fig. 5 agree qualitatively with those obtained by Blokhina and Ordanovich [6] who examined convection on the background of small-scale turbulence, aimed at studying the Langmuir circulations (lower effective Rayleigh and Prandtl numbers were used there). Note that the temperature on the layer bottom was fixed in [6], which results in heat inflow from the lower boundary of the layer and establishment of steady-state rolls.

Conclusions. Evolution of convective structures formed in a cavity of small volume filled by liquid (ethanol) under an airflow with increasing velocity is studied. A transition from hexagonal cells to streamwise convective rolls is found. Evaporation of the liquid in the presence of convective structures leads to a decrease in liquid temperature to a constant value.

Evolution of two-dimensional rolls is studied theoretically and numerically. It is demonstrated that the main effect on the limiting temperature in the cooled layer under the test conditions used is exerted by the dependence of saturated vapor density on temperature. The calculations prove that the boundary conditions for an oscillating flow on the surface of the liquid layer can be replaced, without losing accuracy, by simpler relations, which do not require the oscillating fields in air to be calculated.

The main specific features of the flow typical of the experiments performed are determined within the framework of the numerical solution of the problem. It is shown that convective structures play an important role in formation of a thin temperature boundary layer near the surface.

This work was supported by the Russian Foundation for Basic Research (Grant No. 04-05-64627).

REFERENCES

1. A. S. Monin and V. P. Krasitskii, *Phenomena on the Ocean Surface* [in Russian], Gidrometeoizdat, Leningrad (1985).
2. G. N. Panin, *Heat and Mass Transfer between the Water Basin and Atmosphere under Natural Conditions* [in Russian], Nauka, Moscow (1985).
3. K. N. Fedorov and A. I. Ginzburg, *Subsurface Layer of the Ocean* [in Russian], Gidrometeoizdat, Leningrad (1988).
4. V. I. Polezhaev, A. V. Bune, N. A. Verezub, et al., *Mathematical Modeling of Convective Heat and Mass Transfer by Navier–Stokes Equations* [in Russian], Nauka, Moscow (1987).
5. V. A. Shlychkov, "Estimate of the influence of a "cold surface film" in modeling convection in a water basin," *Vychisl. Tekhnol.*, **3**, No. 6, 97–105 (1998).
6. N. S. Blokhina and A. E. Ordanovich, "Mathematical modeling of vortex structures in the upper layer of the ocean," *Izv. Ross. Akad. Nauk, Fiz. Atmos. Okeana*, **3**, No. 5, 686–695 (1994).
7. M. Tveitereid and H. W. Müller, "Pattern selection at the onset of Rayleigh–Benard convection in a horizontal shear flow," *Phys. Rev. E*, **20**, No. 2, 1219–1226 (1994).
8. A. B. Ezersky and V. V. Chernov, "Effect of wind stresses on the structure of convection in a liquid layer heated from below," *Izv. Ross. Akad. Nauk, Fiz. Atmos. Okeana*, **35**, No. 5, 656–659 (1999).
9. A. B. Ezersky, A. V. Nazarovskii, and V. V. Chernov, "Effect of wind stresses on convective structures in a liquid layer heated from below," *Izv. Ross. Akad. Nauk, Ser. Fiz.*, **64**, No. 12, 2397–2404 (2000).
10. A. B. Ezersky, V. P. Reutov, G. V. Rybushkina, and V. V. Chernov, "Simulation of the convective structures in a thin liquid layer in the presence of a wind-driven flow," in: *Frontiers of Nonlinear Physics*, Proc. of the 2nd Int. Conf., Inst. of Applied Physics, Russian Acad. of Sci., Nizhny Novgorod (2005), pp. 243–247.
11. Y. A. Papadimitrakis, E. Y. Hsu, and E. L. Street, "On the structure of the velocity field over progressive mechanically-generated water waves," *J. Phys. Oceanogr.*, **14**, 1937–1947 (1984).
12. A. V. Getling, *Rayleigh–Benard Convection. Structures and Dynamics*, World Scientific, Singapore (1997).
13. G. K. Batchelor, *Introduction to Fluid Dynamics*, Cambridge Univ. Press, Cambridge (1967).
14. V. A. Akulichev, V. N. Alekseev, and V. A. Bulanov, *Periodic Phase Changes in Fluids* [in Russian], Nauka, Moscow (1986).
15. L. D. Landau, A. N. Akhiezer, and E. M. Lifshits, *Course of General Physics. Mechanics and Molecular Physics* [in Russian], Nauka, Moscow (1965).
16. L. D. Landau and E. M. Lifshits, *Course of Theoretical Physics*, Vol. 6: *Fluid Mechanics*, Pergamon Press, Oxford-Elmsford, New York (1987).